HHS Public Access

Author manuscript

Brain Struct Funct. Author manuscript; available in PMC 2020 November 01.

Published in final edited form as:

Brain Struct Funct. 2020 May ; 225(4): 1313–1326. doi:10.1007/s00429-020-02060-3.

Spatial organization of occipital white matter tracts in the common marmoset

Takaaki Kaneko[1,*], **Hiromasa Takemura**[2,3,*], **Franco Pestilli**[4], **Afonso C. Silva**[5], **Frank Q. Ye**[6], **David A. Leopold**[6,7]

[1)]RIKEN Center for Brain Science (CBS), Wako-shi, Japan

[2)]Center for Information and Neural Networks (CiNet), National Institute of Information and Communications Technology, and Osaka University, Suita-shi, Japan

[3)]Graduate School of Frontier Biosciences, Osaka University, Suita-shi, Japan

[4)]Department of Psychological and Brain Sciences, Indiana University, 1101 E 10th Street, Bloomington IN 47405, USA

[5)]Department of Neurobiology, University of Pittsburgh Brain Institute, University of Pittsburgh, Pittsburgh, PA, USA

[6)]Neurophysiology Imaging Facility, National Institute of Mental Health, National Institutes of Neurological Disorders and Stroke, National Eye Institute, National Institutes of Health, Bethesda, MD, USA

[7)]Laboratory of Neuropsychology, National Institute of Mental Health, National Institutes of Health, Bethesda, MD, USA

Abstract

The primate brain contains a large number of interconnected visual areas, whose spatial organization and intracortical projections show a high level of conservation across species. One fiber pathway of recent interest is the vertical occipital fasciculus (VOF), which is thought to support communication between dorsal and ventral visual areas in the occipital lobe. A recent comparative diffusion MRI (dMRI) study reported that the VOF in the macaque brain bears a similar topology to that of the human, running superficial to and roughly perpendicular to the optic radiation. The present study reports a comparative investigation of the VOF in the common marmoset, a small New World monkey whose lissencephalic brain is approximately 10-fold smaller than the macaque and 150-fold smaller than the human. High-resolution *ex vivo* dMRI of

Corresponding authors: Takaaki Kaneko, RIKEN Center for Brain Science (CBS), 2-1 Hirosawa, Wako-shi, Saitama 351-0198 Japan, takaaki.kaneko@riken.jp, +81-48-467-5973; Hiromasa Takemura, Center for Information and Neural Networks (CiNet), National Institute of Information and Communications Technology, and Osaka University, 1-4 Yamadaoka, Suita-shi, Osaka 565-0871 JAPAN, htakemur@nict.go.jp, +81-80-9098-3285.

*These authors contributed equally to this work

Competing financial interest: The authors declare no competing financial interests associated with this article.

Compliance with ethical standards

Research involving human participants: Data collection from human participants was approved by the Institutional Review Boards (IRBs) of the University of Washington, Saint Louis (HCP data set).

Informed consent: All participants provided written informed consent to participate in the project.

two marmoset brains revealed an occipital white matter structure that closely resembles that of the larger primate species, with one notable difference. Namely, unlike in the macaque and the human, the VOF in the marmoset is spatially fused with other, more anterior vertical tracts, extending anteriorly between the parietal and temporal cortices. We compare several aspects of this continuous structure, which we term the VOF complex (VOF+), and neighboring fasciculi to those of macaques and humans. We hypothesize that the essential topology of the VOF+ is a conserved feature of the posterior cortex in anthropoid primates, with a clearer fragmentation into multiple named fasciculi in larger, more gyrified brains.

Keywords

comparative anatomy; visual cortex; diffusion MRI; white matter; vertical occipital fasciculus; marmoset

Introduction

The cerebral cortex of primates contains a shared mosaic of visual areas, which reflect primates' dependence on vision for social behavior, manual actions, and movement through the environment (Mitchell and Leopold 2015; Leopold et al. 2017; Kaas 2013). These cortical areas are interconnected through a meshwork of white matter fiber tracts, many of which have been studied extensively using diffusion-weighted magnetic resonance imaging (dMRI) in humans. Among primates, the anatomical and functional layout of large brains (e.g. humans) and small brains (e.g. marmosets) is known to be broadly similar (Solomon and Rosa 2014; Zhu and Vanduffel 2019). Larger brains may have more cortical areas, possibly due to brain scaling itself (Kaas 2013; Van Essen and Glasser 2018), though the precise homology of areas between different primate species is an ongoing topic of discussion (Tootell et al. 2003; Rosa and Tweedale, 2005; Wandell and Winawer 2011; Lyon and Connolly 2012). Primate brains of different sizes also differ in their gyrification, which is known to affect the segregation of long-range fasciculi (Zilles et al., 1989; 2013; Rademacher et al. 1993; Rogers et al., 2010). Both parcellation and gyrification of the cortex are closely related to the structure of the underlying white matter. Gyrification, for example, can severely affect the complexity of fibers trajectories just beneath the cortex, leading to an uneven detectability of cortical connections (Reveley et al. 2015). Nonetheless, comparative studies of the cerebral white matter have begun to shed light on homologies across species, and the principles underlying the complex white matter organization in the human brain (Croxson et al., 2005; Schmahmann et al. 2007; Rilling et al., 2008; Jbabdi et al. 2013; Schaeffer et al., 2017; Takemura et al. 2019; Thiebaut de Schotten et al. 2012; 2019).

Recently, there has been a growing effort to understand the organizational principles of white matter pathways connecting the human parietal, occipital and temporal cortex (Catani et al., 2005; Menjot de Champfleur et al., 2013; Yeatman et al. 2014; Takemura et al. 2016b; Markis et al., 2017; Weiner, Yeatman, Wandell, 2016; Bullock et al., 2019). For example, one study applied a comparative approach to dMRI and tractography data in the macaque and human to examine the anatomical features of dorsoventrally running occipital white matter pathways (Takemura et al. 2017). That study demonstrated a high level of

conservation across the two species but also identified some pronounced distinctions in the segregation of fasciculi. For example, one pair of prominent white matter tracts, the inferior longitudinal fasciculus (ILF) and the vertical occipital fasciculus (VOF) were segregated in the human brain but conjoined in the macaque. While such differences may reflect genuine connectional differences acquired through evolution, an interesting prospect is that they are merely a reflection of gyrification and have minimal bearing intracortical connectivity. One potentially fruitful avenue to further investigate the relative effects of brain size and phylogeny is to compare these results to those obtained in a much smaller primate brain.

Here we investigate the occipital white matter pathways in the common marmoset (*Callithrix jacchus*), a New World monkey that diverged from humans approximately 40 million years ago and which represents one of the smallest simian primates. With a small brain (<8g) that is lissencephalic (nearly free of gyrification), it lies at the opposite end of the spectrum from the human brain (~1400g) and more than ten-fold smaller than the macaque brain (~100g). Using very high spatial resolution, *ex vivo* diffusion magnetic resonance imaging (dMRI), we asked whether the occipital white matter pathways in this tiny primate brain would resemble those of much larger primates.

We report that the principal features of the occipital pathways are conserved among the three primate species, including the relative positioning of the optic radiation, forceps major, and vertical occipital fasciculus (VOF). The VOF, whose course is perpendicular to the optic radiation, is thought to support communication between dorsal and ventral visual areas (Yeatman et al. 2014; Takemura et al. 2016b). However, unlike in the larger primates, the marmoset VOF appears as a continuous sheet that passes anteriorly into parietal and temporal areas. This continuity sheds new light on the organization of white matter fiber pathways and the potential contribution of gyrification. We discuss these findings in the context of comparative anatomy of cerebral cortex expansion, folding, and functional specialization.

Methods

MR Data acquisition and preprocessing

Marmoset dataset—Two post-mortem *Callithrix jacchus* (common marmoset) brains were imaged using a 30-cm magnet bore Bruker 7T scanner at the National Institutes of Health. Brain sample preparation and acquisition procedure was similar to that used in the macaque study (Reveley et al. 2015). A smaller, 35 mm coil birdcage coil was used to scan the marmoset brain for better sensitivity. The dMRI data were sampled in 126 directions at a spatial resolution of 150 μm isotropic. The b-value was set to 4800 s/mm^2 and echo time (TE) was 34 ms. We note that higher b-value is required for *ex vivo* dMRI acquisition in the marmoset and macaque brains than those typically used for *in vivo* dMRI experiment, since the diffusion coefficient is reduced in post-mortem brains (Sun et al., 2003; Miller et al., 2011; 2012). Six non-diffusion weighted images (b=0) were obtained. Marmoset dMRI data was preprocessed by the TORTOISE software package (Pierpaoli et al. 2010) for eddy-current and motion corrections. The magnetization transfer ratio (MTR) image at 150 μm isotropic resolution was also obtained.

Macaque dataset—This dataset was acquired from a post-mortem *Macaca mulatta* (rhesus macaque monkey) brain using 30-cm magnet bore Bruker 7T scanner at the National Institute of Health. The dMRI data were sampled in 121 directions at a spatial resolution of 250 μm isotropic. The b-value was set to 4800 s/mm^2 and TE was 34 ms. Seven non-diffusion weighted image (b=0) were obtained. The MTR image at 250 μm isotropic resolution was obtained to improve the accuracy of the atlas fitting (Reveley et al., 2016). This dMRI data were analyzed previous publications (Thomas et al. 2014; Reveley et al. 2015; Takemura et al. 2017). Macaque dMRI data was preprocessed by the TORTOISE software package (Pierpaoli et al. 2010) for eddy-current and motion corrections. Processing details were presented previously (Thomas et al. 2014).

Human dataset—We used diffusion-weighted MRI data acquired from three subjects by the Human Connectome Consortium (WU-Minn HCP consortium; Van Essen et al. 2013). The dMRI data were sampled in 90 directions, and the spatial resolution is 1.25 x 1.25 x 1.25 mm^3. TE was 89.5 ms. Measurements from the 2000 s/mm^2 shell were extracted from the original data set and used for analyses because the current implementation of Linear Fascicle Evaluation (Pestilli et al. 2014) that we used only accepts single-shell diffusion MRI data. We also note that HCP dMRI data with b = 2000 s/mm^2 could be relatively closer to *ex vivo* animal dMRI data as compared with HCP dMRI data with b = 3000 s/mm^2 because of a reduction in diffusion coefficient in post-mortem brains (Sun et al., 2003; Miller et al., 2011; 2012). The human dMRI data were preprocessed by the HCP consortium using methods that are presented previously (Sotiropoulos et al. 2013). Whereas the human data used here is from a small number of subjects, the high degree of consistency in the VOF across subjects has already been demonstrated by previous works (Takemura et al. 2016b, 2017; Weiner et al. 2017).

Tractography

We used Ensemble Tractography method to estimate the streamlines from dMRI data (Takemura et al. 2016a). We took this approach using multiple angle threshold in tractography because it has better accuracy for predicting diffusion signal and is less biased in identifying white matter tracts which have different curvature, as compared with tractography with a single parameter selection (Takemura et al., 2016a). Methods used for analyzing human and macaque data were described in a previous publication (Takemura et al. 2017). For marmoset dMRI data, we generated candidate streamlines using constrained spherical deconvolution-based (CSD; L_{max}=10) probabilistic tractography and four angle thresholds (5.7, 11.5, 23.1 and 47.2 deg), implemented in MRtrix3 (Tournier et al. 2012; http://www.mrtrix.org/). We set the minimum streamline length as 10 mm and maximum streamline length as 250 mm. Other parameters were set as default values (step size: 75 μm; Fiber Orientation Distribution Amplitude stopping criterion: 0.05). We used the entire white-matter volume as a seed region and as mask. We generated 2 million streamlines by using each angle threshold and obtained 8 million candidate streamlines in total. Finally, we used Linear Fascicle Evaluation (LiFE; Pestilli et al. 2014; Caiafa and Pestilli 2017; http://francopestilli.github.io/life/) to remove streamlines which do not contribute to predicting dMRI signal.

Tract identification

Marmoset dataset:

Optic Radiation (OR): We identified marmoset optic radiation by selecting streamlines which have one endpoint near the lateral geniculate nucleus (LGN), and the other endpoint near primary visual cortex (V1). The streamlines terminating within 0.2 mm from LGN and V1 are identified as the OR. The location of LGN in individual brains was identified by visual inspection in both (b=0) dMRI and MTR images. The V1 region was identified by fitting histology-based marmoset MRI atlas (Hashikawa et al. 2015; Woodward et al. 2018) and visually confirmed by the presence of the stria of Gennari. Examples of LGN and V1 ROIs are shown in Supplementary Figure 1A–B.

Forceps major: Forceps major was identified as identical criteria as used in a previous macaque dMRI study (Takemura et al. 2017). First, we visually identified corpus callosum ROI in a sagittal slice. Second, we defined two coronal ROIs, one for each hemisphere, which is located posterior to the superior colliculus. Examples of ROIs for identifying forceps major are shown in Supplementary Figure 1C. Forceps major was identified as streamlines passing through all three ROIs.

Vertical Occipital Fasciculus Complex (VOF+): We defined ROI for marmoset VOF+ based on the continuity and discontinuity of diffusion encoding color (DEC) map from dMRI data. This was done because the marmoset brain lacks clear sulcal or gyral landmarks as compared with the human brain and thus it is challenging to make axial waypoint ROI planes with respect to landmarks visible in structural MRI image. More specifically, we identified voxels with superior-inferior diffusion signal that were located between OR and superficial white matter fibers in axial slices. We then drew two waypoint ROIs on the axial planes of those voxels with superior-inferior diffusion signal (blue to purple color in DEC map). We chose two axial slices to draw ROIs, one in dorsal and another in ventral, similar to a previous macaque dMRI study (Takemura et al. 2017). Marmoset VOF+ was then visualized as streamlines passing through both of axial plane ROIs. The position of waypoint ROIs used for identifying marmoset VOF+ is shown in Supplementary Figure 2.

VOF+ subcomponents: In order to make a comparison with human and macaque results, we classified VOF+ streamlines into anterior and posterior portion based on streamline endpoints with respect to cortical areas (see “Cortical area identification in marmoset” below). Streamlines with endpoints near (within 200 μm) dorsal occipital cortices (DM/V6, DA/V3A, A19DI, V6a) was categorized as posterior VOF+, while streamlines terminate near parietal cortices (PE, PEC, PG, MIP, VIP, LIP, AIP, OPt) were categorized as anterior VOF+.

Human and macaque dataset

In human and macaque, occipital white matter tracts (OR, forceps major and VOF) were identified by a waypoint ROI approach as described in a previous publication (Takemura et al. 2017).

In addition, we further identified a tract (pAF) in human and macaque connecting parietal and inferotemporal cortex. We used AFQ VOF toolbox (https://github.com/jyeatman/AFQ/tree/master/vof) in the human data to identify pAF from whole-brain streamlines (see Yeatman et al., 2014; Weiner et al., 2016 for details). In the macaque data, we manually defined two axial waypoint ROIs and identified putative pAF as streamlines passing through both of ROIs. We describe the positions of ROIs used to identify this tract in Supplementary Figure 3.

Outlier streamline removal

For all datasets, we refined tract identification by removing outlier streamlines using the following criteria: 1) the streamline length was ≥3 SD longer than the mean streamline length in the tract, 2) the streamline position was ≥3 SD away from the mean position of the tract (Yeatman et al. 2012). For the VOF/VOF+, streamlines whose path deviated more than 2 SD from the mean direction of the VOF streamlines were also discarded as in the previous study (Takemura et al. 2016b).

Evaluating of microstructural properties along the tract

We evaluated the microstructural properties of each white matter tract based on methods used in previous studies (Levin et al. 2010; Yeatman et al. 2012; Ogawa et al. 2014; Duan et al. 2015; Rokem et al., 2017; Yoshimine et al., 2018). Briefly, we first calculated fractional anisotropy (FA; Basser and Pierpaoli 1996) in all voxels by fitting diffusion tensor model to dMRI data collected from each species. Second, we resampled each streamline belong to the tract of interests (OR, forceps major, and VOF/VOF+) to 100 equidistant nodes. Tissue properties were calculated at each node of each streamline using a spline interpolation of FA values. The properties at each node were summarized by taking a weighted average of FA values on each streamline within that node. The weight of each streamline was based on the Mahalanobis distance from the tract core. We excluded the first and last 15% of the nodes from the tissue property of the tract core to exclude voxels close to gray/white matter interface where the tract was likely to be intersect heavily with the other fibers, such as superficial U-fiber system (Ogawa et al. 2014; Reveley et al. 2015; Duan et al. 2015). We summarized the profile of each tract with a vector of 70 values representing the FA measurements sampled at equidistant locations along the central portion of the tract. We averaged FA measurements among all 70 nodes to obtain a single-number summary for each tract. We compared microstructural properties (FA) across the tract in each species, and then evaluated how those microstructural similarities were preserved across species.

Cortical area identification in marmoset

We identified cortical areas in the marmoset brain by incorporating a histology-based marmoset brain atlas, initially proposed by Hashikawa and colleagues (Hashikawa et al. 2015; Woodward et al. 2018). In this atlas, the border between cortical areas are defined by comparison between histological measurement and MRI, and thus the atlas is defined in a stereotactic coordinate system. We used non-linear registration method implemented in Advanced Normalization Tools (ANTs; Avants et al. 2014; http://stnava.github.io/ANTs/) to register atlas brain into individual marmoset brain. We used atlas ROI transformed into individual marmoset brain space for subsequent analyses.

Estimation of cortical tract endpoints in marmoset dMRI data

Streamlines terminate at the boundary between white and gray matter. We measured the distance between tract endpoints and gray matter voxels to identify the cortical areas closest to the tract endpoints. Specifically, we collected the coordinates of the endpoints of the VOF + streamlines and computed the distance between the coordinates of the endpoint and gray matter voxels. Then, for each gray matter voxel, we counted the number of endpoints within a threshold distance (750 μm). We plotted the normalized endpoint counts (normalized to the maximum endpoint counts in each hemisphere) on the smoothed cortical surface in individual hemisphere first, and then transformed it into the atlas space (Hashikawa et al., 2015). We visualized the mean endpoint counts across four hemispheres from two marmoset brains on the smoothed cortical surface of the atlas wth cortical parcellation (Figure 4A). Endpoint coverage of each cortical area was calculated as a ratio of vertex where normalized endpoint counts are more than 0.05 to the total vertex of each cortical area (Figure 4B). This analysis has known limitations, derived from challenges in associating the cortical surface and tract endpoints (Reveley et al. 2015). We thus applied this method to estimate the regional proximity of the white matter tracts to known cortical areas, acknowledging that precise gray matter connections could not be determined.

Results

The aim of this study was to compare the macroscale spatial organization of major occipital white matter tracts in the marmoset brain, with those in the human and macaque, using dMRI-based tractography. The following sections describe the approach we took to achieve this comparison, first identifying the extents of the major tracts through inspection of the DEC map and then applying tractography to compare both macroscale organization and intrinsic fiber properties of the occipital white matter across species.

Spatial organization of marmoset occipital white matter tracts

dMRI tractography studies utilize anatomical knowledge obtained from invasive studies to apply reasonable constraints to the identification of white matter tracts (Catani et al. 2002; Wakana et al. 2004; Schmahmann and Pandya 2006; Schmahmann et al. 2007). As a first step, and before applying tractography methods below, we investigated the segmentation of the occipital white matter through inspection of the local orientation information via the DEC map (Pajevic and Pierpaoli 1999).

Figure 1 depicts the DEC map obtained from high-resolution *ex vivo* marmoset dMRI dataset (see Methods; see Takemura et al. 2017 for examples from macaque and human). Three principal white matter bundles are clearly visible in DEC map of the marmoset occipital lobe (Figure 1; see Supplementary Figure 4A for DEC map in another marmoset brain). Two of these bundles are apparent homolog of the optic radiation (OR) and forceps major, respectively. The OR is located in the deep occipital white matter with predominantly anterior-posterior diffusion direction (green color in Figure 1). The anterior portion of this bundle is located close to the LGN, and the posterior portion is located near the calcarine sulcus, which corresponds to V1. The second primary bundle is forceps major, which is a bundle of callosal fibers connecting the left and right occipital lobes. On the DEC map, the

forceps major is particularly visible at the corpus callosum, as voxels with predominantly left-right diffusion direction (red). The third bundle was laterally (i.e. superficially) adjacent to the OR and running dorsal-ventral direction as indicated by principal diffusion direction in the superior-inferior axis (blue). This third bundle in the marmoset is apparently similar to the vertical occipital fasciculus (VOF) reported in human and macaque (Yeatman et al. 2014; Takemura et al. 2017, 2018), as we discuss in later sections. We were not able to address the comparative organization of subtler white matter organization, such as the short-range U-fibers, since the data from the different species were collected with different acquisition parameters and voxel sizes (see Methods).

In sum, visual inspection of the DEC map clearly shows that the fiber structures in marmoset occipital white matter are highly organized, with multiple sheet-like fascicles along the lateral-medial axis. In spite of its diminutive brain size and lack of complex gyrification when compared to other primate species, the essential fiber organization of the marmoset brain is highly similar to that of the macaque and human.

Comparison of major occipital white matter tracts across human, macaque and marmoset

We next performed tractography to estimate three-dimensional trajectories of major occipital white matter tracts visible in DEC maps. Figure 2 shows tractography of the three principal white matter structures described above in the marmoset, macaque and human brains (see Methods; Supplementary Figure 4B for results in another marmoset brain).

The topological configuration of principal occipital bundles, such as the OR (green in Figure 2) and forceps major (dark yellow in Figure 2), was shown to be highly similar across the species. Consistent with the superficial, dorsoventrally running white-matter region observed in the DEC map, we identified a sheet-like bundle of track lines running just lateral to, and roughly perpendicular to, the OR (blue in Figure 2). This pathway, named the vertical occipital fasciculus (VOF) in the human and macaque, was known to classical anatomists and recently re-discovered through dMRI-based tractography (Yeatman et al. 2013; 2014; Takemura et al. 2017, 2019).

In the marmoset brain, a large, vertically oriented sheet of occipital fibers was particularly conspicuous and coherent. Whereas the posterior portion of this large fasciculus appeared to correspond topologically to the VOF of the larger species, the anterior portion of the fiber sheet extended further into the parietal and temporal cortices than in the macaque and human (Weiner et al., 2016; Panesar et al., 2019; Bullock et al., 2019; Schurr et al., 2019). Given this difference, we termed this white matter structure in the marmoset the vertical occipital fasciculus *complex* (VOF+). We next investigated this structure in more detail.

Microstructural comparison of occipital white matter

We next compared the fractional anisotropy (FA; Basser and Pierpaoli 1996) of three prominent white matter tracts in the three primate species. Since dMRI data was collected in different scanners and under different acquisition parameters and resolution and conditions (*in vivo* human vs. *ex vivo* monkeys), we did not attempt to compare the absolute FA values across species. Nonetheless, the *relative* FA indices are thought to be largely preserved in

post-mortem brains (Sun et al., 2003), thus we compared this value in the OR, VOF, and forceps major in the three species.

Figure 3A depicts the DEC map and FA map for a representative axial slice from the marmoset, macaque and human brains. Although baseline FA measurements differed across datasets due to voxel size and other factors, the relative FA values across occipital pathways were similar across species. In all three primate species, the forceps major has the highest FA values. It was also commonly observed that FA value in OR was higher than the VOF/VOF+. This observation is consistent with findings from histological studies showing that OR is more myelinated as compared with the VOF (Vogt 1904; Yeatman et al. 2014; Takemura et al. 2019). Figure 3B describes a summary of FA (average along each tract) in each species, and again relative FA values across occipital tracts are consistent across species.

In sum, we observed that three major occipital tracts were similar across species, not only in three-dimensional topology observed in tractography, but also in voxelwise microstructural measurements. A consistent finding of microstructure difference between OR and VOF+ further supports the view that the marmoset VOF+ is similar to VOF in macaque and human.

Putative cortical endpoints of marmoset VOF+

One of the intriguing aspects of the VOF is its implications for functional processing within the visual pathway, providing an explicit path for interactions between dorsally and ventrally located visual areas. While such cortico-cortical connections are known to exist (Petr et al. 1949; Seltzer and Pandya 1984; Clarke 1994; Schmahmann and Pandya 2006; Ungerleider et al. 2008), they have attracted less attention as compared with the more prominent anteroposterior pathways that shape the parallel dorsal and ventral streams (Morel and Bullier 1990; Wallisch and Movshon 2008). In the macaque and humans, VOF has been hypothesized to be crucial for transmitting signals between regions that analyze object property and regions that map spatial information (Takemura et al. 2016b). Although it is known that dMRI-based tractography has a fundamental limitation in precisely determining gray matter connections (Reveley et al. 2015), it is possible to make plausible estimations of regional connectivity based on the endpoints of tract streamlines. Here we tested whether marmoset VOF+ shares a pattern of regional connectivity with the VOF of the macaque and human, which would point to a similar functional role of these pathways.

In Figure 4A–B, these estimates are presented on the surface of the marmoset cortex, using a histology-based marmoset brain atlas for reference (Hashikawa et al., 2015; Woodward et al., 2018). We found that the dorsal endpoints of the VOF+ were near cortical areas DM (V6), DA (V3A) and PPm (V6), and ventral endpoints were near VLA (V4) and ITc (TEO). These observations support the idea that the VOF+ serves to transmit visual information across relatively early stages of the dorsal and ventral visual streams, which is qualitatively consistent with the observation in human and macaque (Takemura et al., 2017; see Supplementary Figure 5).

However, as mentioned above, one notable difference with the other species is that the posteroanterior extent of the marmoset VOF+ is broad and uninterrupted, extending into the

parietal and temporal cortex. Dorsal endpoints of VOF+ was observed not only at dorsal occipital cortices but also posterior parietal region such as LIP, MIP and Opt. Similar to dorsal endpoints, ventral endpoints also extended to broader areas than that of macaque and human. A substantial gathering of track endpoints was found at regions along superior temporal sulcus (e.g., FST) and inferior temporal cortex (TE3).

This analysis shows that the posterior portion of the marmoset VOF+ has a similar connectional motif to the VOF of macaque and human (Takemura et al. 2017; see Discussion), but that the more anterior aspects more likely correspond to other tracts manifested as multiple different bundles in larger primates. In the next section, we seek potential candidates of such fasciculi to gain insights into potential homologies.

Continuity of the marmoset VOF+ fiber sheet

The sheet of fibers identified as VOF+ exhibited a broad and continuous set of endpoints that spanned multiple cortical regions dorsally and ventrally, extending anteriorly beyond the occipital VOF profile in the other two species (see Takemura et al., 2017). Human anatomical and diffusion MRI studies have demonstrated that the VOF and posterior arcuate fasciculus (pAF) can be clearly distinguished as distinct fasciculi. The VOF connects the dorsal and ventral occipital cortex whereas pAF connects parietal cortex and inferotemporal cortex (Curran 1909; Catani et al. 2005; Martino and Garcia-Porrero 2013; Weiner et al. 2017; Yeatman et al. 2014; Takemura et al. 2016b; Lerma-Usabiaga et al., 2018; Budisavljevic et al. 2018; Bullock et al., 2019; Panesar et al. 2019; Schurr et al., 2019). In macaque, a recent dMRI study also distinguished the VOF from a more anterior tract and connecting parietal and inferotemporal cortex (Sani et al. 2019). Might the anterior aspects of the marmoset VOF+ correspond to these sheets identified in the other species?

To address this question, we first examined the fiber pathways anterior to the VOF in the macaque and human. We identified a pathway connecting parietal and inferotemporal cortex from macaque dMRI data (magenta in Figure 5A, middle panel; see Methods). This tract is physically separated and distinguishable from VOF (blue), as two tracts are divided by the superior temporal sulcus. In this paper, we term this tract as putative pAF in macaque (also termed as vertical inferior longitudinal fasciculus, Sani et al. 2019). Thus, similar to the conclusions from human dMRI (Figure 5A, bottom panel), macaque dMRI supports the distinction between VOF and putative pAF.

This clear distinction was absent in the marmoset, as there were no apparent boundaries within VOF+ in marmosets. Nonetheless, we investigated a potential division of VOF+ into anterior and posterior part based on dorsal cortical endpoints of VOF+ streamlines (see Methods). Namely, we classified VOF+ streamlines having endpoints near posterior parietal cortex as anterior VOF and streamlines having endpoints near dorsal occipital cortex as posterior VOF+. Using this method, we did not find evidence for segregation between anterior and posterior segments of VOF+ to match the other species (Figure 5A, top panel). In fact, the anterior and posterior VOF+ streamlines overlapped with each other in about 48% (49% and 48% for marmoset1 and marmoset2, respectively) of white matter voxels along the trajectory, which was much more extensive than in the macaque and human (Figure 5B).

Discussion

Over the last decade, a number of dMRI studies investigated spatial organization of white matter tracts in humans and macaques (Catani et al. 2002, 2017; Wakana et al. 2004; Schmahmann et al. 2007; Rilling et al. 2008; Jbabdi et al. 2013; Yeatman et al. 2014; Mars et al. 2016; Takemura et al. 2017). The complex gyrification in human and macaque brain often make it difficult to understand basic topological organization of connections, which is thought to be preserved across species. Since the marmoset brain has minimal sulcal folding, this species offers a chance to observe white matter motifs that are also present in larger primate species such as the human, but whose basic topology may be obscured because of excessive gyrification.

This study demonstrates that the spatial organization of the three major occipital white matter tracts (OR, forceps major and VOF) are similar across the marmoset, macaque and human. In particular, the vertical occipital fasciculus is conspicuous in the common marmoset and is therefore likely to have been present in the earliest anthropoid primates. Similar to the macaque and human, the VOF+ in the marmoset brain occupies the occipital lobe, running just lateral, and roughly perpendicular, to the OR. It differs from the VOF in the other species, however, in that it is a continuous sheet structure that extends significantly further into the parietal and temporal lobes. We discuss the VOF, its putative function, and the implications of the observed species differences below.

Visual field representation and VOF/VOF+ endpoints

The VOF connects well-studied regions of the primate visual cortex but was largely ignored in the neuroscience community until its recent re-discovery in dMRI studies (Yeatman et al. 2013; 2014; Takemura et al. 2017). Its role in visual processing remains speculative. In the human and macaque, visual areas V2 and V3 are split into quarter-field representations, with lower visual field positioned dorsally and upper visual field positioned ventrally (Wandell and Winawer 2011; Lyon and Connolly 2012). While the retinotopic mapping in areas anterior to V3 has been often debated among investigators, most areas show complete hemifield representations (Smith et al. 1998; Press et al. 2001; Wade et al. 2002; Brewer et al. 2005; Winawer et al. 2010; Kolster et al. 2014; Arcaro and Livingstone, 2017; Zhu and Vanduffel 2019). Previous studies in both humans and macaques proposed that the VOF serves to connect complete hemifield visual field maps situated in the dorsal and ventral visual cortex, and thus has a vital role in transmitting both upper and lower visual field information (Takemura et al. 2016b, 2017; Rokem et al., 2017; Schurr et al., 2019; Jitsuishi et al., 2020).

The VOF+ identified in the marmoset is consistent with this hypothesis, since VOF+ streamlines terminate near area DA (V3A), DM (V6) dorsally and ITC (TEO) ventrally (Figure 4). According to previous physiological and anatomical studies, these areas in marmoset also represent complete hemifield (Rosa and Tweedale 2005; Jeffs et al. 2013; Solomon and Rosa 2014; Angelucci and Rosa 2015). Consistent with this idea, a previous tracer study reported that a part of dorsal area DM with upper visual field representation is connected to ventral extrastriate areas (ventral V2, V3 and V4; Rosa et al., 2009). Such visual field-specific connections between dorsal and ventral extrastriate areas are likely a

part of VOF+. Thus, similar to the VOF in the other two species, the posterior portions of the VOF+ in the marmoset are likely to transmit both upper and lower visual field information to areas containing full hemifield representations.

Inter-species differences in parietotemporal fasciculi

The larger than expected anterior extent of the marmoset VOF+ raises questions about homological correspondence, with current evidence suggesting that the marmoset VOF+ corresponds to the VOF together with the pAF in the larger, more gyrified primate species. Classical and dMRI anatomical studies in humans have readily distinguished the VOF from the pAF, which connects parietal and inferotemporal cortex (Curran 1909; Catani et al. 2005; Martino and Garcia-Porrero 2013; Weiner et al. 2017; Lerma-Usabiaga et al., 2018; Budisavljevic et al. 2018; Panesar et al. 2019; Schurr et al., 2019). Human pAF has been considered to have endpoints near inferior parietal lobule dorsally and posterior and middle temporal lobe ventrally (Bullock et al., 2019), although the exact cortical terminations of human pAF in relation with detailed cortical parcellation has not been established. In the macaque, tracer-based autoradiography studies reported fiber tracts connecting parietal cortex and inferotemporal cortex (Seltzer and Pandya 1984; Cavada and Goldman-Rakic 1989; Schmahmann and Pandya 2006). According to these observations, this vertical fiber bundle runs orthogonal to the OR, terminating dorsally in the parietal cortex and ventrally in areas near the occipitotemporal sulcus. A recent dMRI study in the macaque further reported this pathway serves to a connection between LIP and posterior inferotemporal cortex (Sani et al. 2019). That study discussed putative homology of this fasciculus, previously considered a portion of the ILF, to human pAF (See Supplemental results for marmoset ILF and Supplementary Figure 6). They further demonstrated highlighted the clear distinction between pAF and VOF, consistent with our findings in the macaque (Figure 5).

In the marmoset, where there is no obvious fasciculation of the pAF, the anterior part of marmoset VOF+ has endpoints near parietal areas LIP, MIP, VIP and OPt dorsally, areas TEO and TE ventrally (Figure 4). These endpoints are roughly match the endpoints of the pAF in the macaque (Sani et al. 2019). Thus a parsimonious interpretation of the marmoset data is that the VOF+ corresponds to a juxtaposition of VOF and pAF fasciculi in the other species, which form a continuous sheet in the marmoset owing to the near absence of sulcal folds.

At the same time, we cannot exclude the possibility that adaptive connectional reorganization contributes to the observed differences. In human and macaque studies, the role of VOF and pAF has been discussed in the context of different functional circuitry, such that VOF has been discussed for integration between upper and lower visual field in extrastriate visual field maps (Takemura et al. 2016b) while pAF has been discussed for reading (Thiebaut de Schotten et al. 2014), action-to-object coordination (Budisavljevic et al. 2018) or communication between attention networks (Sani et al. 2019). As diffusion MRI datasets achieve higher spatial resolution (Liu et al. 2020) that allow for the disambiguation of crossing fibers (Roebroeck et al., 2008), it may eventually be possible to distinguish subcomponents within the marmoset VOF+.

Finally, human and macaque studies have also reported other fiber bundles connecting parietal and temporal cortex, such as middle longitudinal fasciculus (MdLF; Schmahmann and Pandya, 2006; Schmahmann et al., 2007; Markis et al., 2009; Wang et al., 2013; Maldonado et al., 2013) and a so-called temporoparietal connection (TP; Kamali et al., 2014; Wu et al., 2016). These tracts have been distinguished from pAF in humans since their cortical endpoints can be distinguishable from those of pAF with respect to cortical sulcus folding (Bullock et al., 2019). Since the marmoset brain lacks complex gyrification, it is possible that additional fibers, corresponding to human MdLF or TP, also run through the VOF+ and could not be distinguished from occipital dorsal-ventral connections as a separate bundle.

Advantage of studying connectional motifs in a smooth brain

One interesting prospect coming from this study is that certain white matter connectional motifs are more visible in the lissencephalic marmoset compared to the macaque and human. Cortical sulci are known to affect, and possibly distort, the course of white matter fiber pathways (e.g. branches of human superior longitudinal fasciculus; Thiebaut de Schotten et al., 2011). The continuity of vertical tracts observed in the marmoset may reflect the topological continuity of the natural fiber growth pattern in this part of the brain, and one that is obscured in gyrencephalic brains. This regularity of fiber patterning within the marmoset may aid in the difficult task of understanding the principles intracortical connectivity in the primate brain. The VOF+ connections seem particularly relevant for one prominent feature of the primate visual cortex, namely its division into functionally segregated dorsal and ventral visual pathways (Ungerleider and Mishkin, 1982; Goodale and Milner, 1992; Wallisch and Movshon 2008). While it is known that these pathways do have routes of anatomical communication (Morel and Bullier 1990), the prominence of the VOF+ sheds new light on the completeness of their interconnection. The uninterrupted nature of this dorsoventral sheet is striking. It is interesting to consider that, even in gyrified primate brains, this sheet may be best conceived as continuous, with its developmental segregation into distinct bundles being less important than its overall continuity. It bears emphasis that this interpretation is speculative: other factors, such as allometric scaling associated with overall brain size and the functional specialization associated with species selective adaptations, can also contribute to the higher level of segregation in the larger primates. Comparison of a more extensive number of species (Thiebaut de Schotten et al. 2019) may be an essential approach to address this question in the future.

It is notable that the major fiber pathways we observed ran in largely orthogonal orientations. Wedeen and colleagues (2012) proposed that one of the collective organization principles in white matter across primate species is that grid structures which are composed by orthogonally crossing two independent fascicles. We indeed observe some similar structures, such that VOF (VOF+) streamlines located lateral and orthogonal to OR streamlines in marmoset, macaque and humans, in some ways consistent with a grid-like organization at a macro-scale level, though the fundamental nature of this organization is still a topic of debate (Catani et al. 2012; Tax et al. 2016).

Conclusion

In this study, we analyzed dMRI dataset from common marmosets to compare the spatial organization of major occipital white matter tracts across primate species. We found that there is a common spatial organization among optic radiation and VOF among humans, macaques and marmosets, suggesting that a key organization principle may be present at common anthropoid primate ancestor. The microstructural profile of major occipital white matter tract is also similar across species. However, the marmoset VOF+ is a continuous sheet structure including fibers connecting parietal and inferotemporal cortex, which are categorized as a distinct bundle in humans and macaques. This difference may be attributed to the difference in brain size or relative cortical folding, whereby the same basic connectional pattern is fragmented into distinct fasciculi in the larger, more gyrified brains.

Supplementary Material

Refer to Web version on PubMed Central for supplementary material.

Acknowledgments:

This work was supported by Japan Society for the Promotion of Science (JSPS) KAKENHI (JP15K16015 and JP19K20653, T.K; JP15J00412 and JP17H04684, H.T), the program for Brain Mapping by Integrated Neurotechnologies for Disease Studies (Brain/MINDS) from the Japan Agency for Medical Research and Development (AMED). D.A.L. and F.Q.Y. are supported by the Intramural Research Program of the National Institute of Mental Health (ZIC MH002899). F.P. was supported by NSF IIS-1636893, NSF BCS-1734853, NSF IIS-1912270 and NSF AOC 1916518, a Microsoft Investigator Fellowship. A.C.S. was supported by the Intramural Research Program of the National Institute of Neurological Disorders and Stroke (ZIA NS003041). Human dMRI data used to produce the figure in this article were provided by the Human Connectome Project, WU-Minn Consortium (Van Essen, D. and Ugürbil, K., 1U54MH091657).

References

Angelucci A, Rosa MGP (2015) Resolving the organization of the third tier visual cortex in primates: a hypothesis-based approach. Vis Neurosci 32:E010 [PubMed: 26241792]

Arcaro MJ, Livingstone MS (2017) Retinotopic organization of scene areas in macaque inferior temporal cortex. J Neurosci 37:7373–7389 [PubMed: 28674177]

Avants BB, Tustison NJ, Stauffer M, et al. (2014) The Insight ToolKit image registration framework. Front Neuroinform 8:44 [PubMed: 24817849]

Basser PJ, Pierpaoli C (1996) Microstructural and physiological features of tissues elucidated by quantitative-diffusion-tensor MRI. J Magn Reson B 111:209–219 [PubMed: 8661285]

Brewer AA, Liu J, Wade AR, Wandell BA (2005) Visual field maps and stimulus selectivity in human ventral occipital cortex. Nat Neurosci 8:1102–1109 [PubMed: 16025108]

Budisavljevic S, Dell'Acqua F, Castiello U (2018) Cross-talk connections underlying dorsal and ventral stream integration during hand actions. Cortex 103:224–239 [PubMed: 29660652]

Bullock DN, Takemura H, Caiafa CF, et al. (2019) Associative white matter connecting the dorsal and ventral posterior human cortex. Brain Struct Funct. 224:2631–2660 [PubMed: 31342157]

Caiafa CF, Pestilli F (2017) Multidimensional encoding of brain connectomes. Sci Rep 7:11491 [PubMed: 28904382]

Catani M, Bodi I, Dell'Acqua F (2012) Comment on "The geometric structure of the brain fiber pathways." Science 337:1605

Catani M, Howard RJ, Pajevic S, Jones DK (2002) Virtual in vivo interactive dissection of white matter fasciculi in the human brain. Neuroimage 17:77–94 [PubMed: 12482069]

Catani M, Jones DK, Ffytche DH (2005) Perisylvian language networks of the human brain. Ann Neurol 57:8–16 [PubMed: 15597383]

Catani M, Robertsson N, Beyh A, et al. (2017) Short parietal lobe connections of the human and monkey brain. Cortex 97:339–357 [PubMed: 29157936]

Cavada C, Goldman-Rakic PS (1989) Posterior parietal cortex in rhesus monkey: I. Parcellation of areas based on distinctive limbic and sensory corticocortical connections. J Comp Neurol 287:393–421 [PubMed: 2477405]

Clarke S (1994) Association and intrinsic connections of human extrastriate visual cortex. Proc Biol Sci 257:87–92 [PubMed: 8090794]

Croxson PL, Johansen-Berg H, Behrens TEJ, et al. (2005) Quantitative investigation of connections of the prefrontal cortex in the human and macaque using probabilistic diffusion tractography. J Neurosci 25:8854–8866 [PubMed: 16192375]

Curran EJ (1909) A new association fiber tract in the cerebrum with remarks on the fiber tract dissection method of studying the brain. J Comp Neurol Psychol 19:645–656

Duan Y, Norcia AM, Yeatman JD, Mezer A (2015) The structural properties of major white matter tracts in strabismic amblyopia. Invest Ophthalmol Vis Sci 56:5152–5160 [PubMed: 26241402]

Felleman DJ, Van Essen DC (1991) Distributed hierarchical processing in the primate cerebral cortex. Cereb Cortex 1:1–47 [PubMed: 1822724]

Goodale MA, Milner AD (1992) Separate visual pathways for perception and action. Trends Neurosci 15:20–25 [PubMed: 1374953]

Hashikawa T, Nakatomi R, Iriki A (2015) Current models of the marmoset brain. Neurosci Res 93:116–127 [PubMed: 25817023]

Jbabdi S, Lehman JF, Haber SN, Behrens TE (2013) Human and monkey ventral prefrontal fibers use the same organizational principles to reach their targets: tracing versus tractography. J Neurosci 33:3190–3201 [PubMed: 23407972]

Jeffs J, Federer F, Ichida JM, Angelucci A (2013) High-resolution mapping of anatomical connections in marmoset extrastriate cortex reveals a complete representation of the visual field bordering dorsal V2. Cereb Cortex 23:1126–1147 [PubMed: 22523183]

Jitsuishi T, Hirono S, Yamamoto T, et al. (2020) White matter dissection and structural connectivity of the human vertical occipital fasciculus to link vision-associated brain cortex. Sci Rep 10**:**820 [PubMed: 31965011] **:**

Kaas JH (2013) The evolution of brains from early mammals to humans. WIREs Cogn Sci 4:33–45

Kolster H, Janssens T, Orban GA, Vanduffel W (2014) The retinotopic organization of macaque occipitotemporal cortex anterior to V4 and caudoventral to the middle temporal (MT) cluster. J Neurosci 34:10168–10191 [PubMed: 25080580]

Kamali A, Sair HI, Radmanesh A, Hasan KM (2014) Decoding the superior parietal lobule connections of the superior longitudinal fasciculus/arcuate fasciculus in the human brain. Neuroscience 277:577–583 [PubMed: 25086308]

Leopold DA, Mitchell JF, Freiwald WA (2017) Evolved mechanisms of high-level visual perception in primates In: Kaas J (ed) Evolution of Nervous Systems, 2nd edition pp 203–235

Lerma-Usabiaga G, Carreiras M, Paz-Alonso PM (2018) Converging evidence for functional and structural segregation within the left ventral occipitotemporal cortex in reading. Proc Natl Acad Sci U S A, 115, E9981–E9990 [PubMed: 30224475]

Levin N, Dumoulin SO, Winawer J, et al. (2010) Cortical maps and white matter tracts following long period of visual deprivation and retinal image restoration. Neuron 65:21–31 [PubMed: 20152110]

Liu C, Ye FQ, Newman JD et al. (2020) A resource for the detailed 3D mapping of white matter pathways in the marmoset brain. Nat Neurosci. [Epub ahead of print]

Lyon DC, Connolly JD (2012) The case for primate V3. Proc Biol Sci 279:625–633 [PubMed: 22171081]

Makris N, Papadimitriou GM, Kaiser JR, et al. (2009) Delineation of the middle longitudinal fascicle in humans: a quantitative, in vivo, DT-MRI study. Cereb Cortex 19:777–785 [PubMed: 18669591]

Markis N, Zhu A, Papadimitriou GM, et al. (2017) Mapping temporo-parietal and temporo-occipital cortico-cortical connections of the human middle longitudinal fascicle in subject-specific, probabilistic, and stereotaxic Talairach spaces. Brain Imaging Behav 11:1258–1277 [PubMed: 27714552]

Maldonado IL, Menjot de Champfleur N, Velut S, et al. (2013) Evidence of a middle longitudinal fasciculus in the human brain from fiber dissection. J Anat 223:38–45 [PubMed: 23621438]

Mars RB, Foxley S, Verhagen L, et al. (2016) The extreme capsule fiber complex in humans and macaque monkeys: a comparative diffusion MRI tractography study. Brain Struct Funct 221:4059–4071 [PubMed: 26627483]

Martino J, Garcia-Porrero JA (2013) In reply: wernicke's perpendicular fasciculus and vertical portion of the superior longitudinal fasciculus. Neurosurgery. 73:E382–E383 [PubMed: 23624415]

Menjot de Champfleur NM, Maldonado IL, Moritz-Gasser S, et al. (2013) Middle longitudinal fasciculus delineation within language pathways: a diffusion tensor imaging study in human. Eur J Radiol 82:151–157 [PubMed: 23084876]

Miller KL, Stagg CJ, Douaud G, et al. (2011) Diffusion imaging of whole, post-mortem human brains on a clinical MRI scanner. Neuroimage 57:167–181 [PubMed: 21473920]

Miller KL, McNab JA, Jbabdi S, Douaud G (2012) Diffusion tractography of post-mortem human brains: optimization and comparison of spin echo and steady-state free precession techniques. Neuroimage 59:2284–2297 [PubMed: 22008372]

Mitchell JF, Leopold DA (2015) The marmoset monkey as a model for visual neuroscience. Neurosci Res 93:20–46 [PubMed: 25683292]

Morel A, Bullier J (1990) Anatomical segregation of two cortical visual pathways in the macaque monkey. Visual Neurosci 4:555–578

Ogawa S, Takemura H, Horiguchi H, et al. (2014) White matter consequences of retinal receptor and ganglion cell damage. Invest Ophthalmol Vis Sci 55:6976–6986 [PubMed: 25257055]

Pajevic S, Pierpaoli C (1999) Color schemes to represent the orientation of anisotropic tissues from diffusion tensor data: application to white matter fiber tract mapping in the human brain. Magn Reson Med 42:526–540 [PubMed: 10467297]

Panesar SS, Belo JTA, Yeh F-C, Fernandez-Miranda JC (2019) Structure, asymmetry, and connectivity of the human temporo-parietal aslant and vertical occipital fasciculi. Brain Struct Funct. 224:907–923 [PubMed: 30542766]

Pestilli F, Yeatman JD, Rokem A, et al. (2014) Evaluation and statistical inference for human connectomes. Nat Methods 11:1058–1063 [PubMed: 25194848]

Petr R, Holden LB, Jirout J (1949) the efferent intercortical connections of teh superficial corten of the temporal lobe (macaca mulatta)*. J Neuropathol Exp Neurol 8:100–103 [PubMed: 18108338]

Pierpaoli C, Walker L, Irfanoglu MO, et al. (2010) TORTOISE: an integrated software package for processing of diffusion MRI data. In: ISMRM 18th annual meeting Stockholm, Sweden

Press WA, Brewer AA, Dougherty RF, et al. (2001) Visual areas and spatial summation in human visual cortex. Vision Res 41:1321–1332 [PubMed: 11322977]

Rademacher J, Caviness VS Jr, Steinmetz H, Galaburda AM (1993) Topographical variation of the human primary cortices: implications for neuroimaging, brain mapping, and neurobiology. Cereb Cortex 3:313–329 [PubMed: 8400809]

Reveley C, Gruslys A, Ye FQ, et al. (2016) Three-dimensional digital template atlas of the macaque brain. Cereb Cortex, 27:4463–4477

Reveley C, Seth AK, Pierpaoli C, et al. (2015) Superficial white matter fiber systems impede detection of long-range cortical connections in diffusion MR tractography. Proc Natl Acad Sci U S A 112:E2820–8 [PubMed: 25964365]

Rilling JK, Glasser MF, Preuss TM, et al. (2008) The evolution of the arcuate fasciculus revealed with comparative DTI. Nat Neurosci 11:426–428 [PubMed: 18344993]

Roebroeck A, Galuske R, Formisano E, et al. (2008) High-resolution diffusion tensor imaging and tractography of the human optic chiasm at 9.4 T. Neuroimage 39:157–168 [PubMed: 17936015]

Rogers J, Kochunov P, Zilles K et al. (2010) On the genetic architecture of cortical folding and brain volume in primates. Neuroimage, 53:1103–1108 [PubMed: 20176115]

Rokem A, Takemura H, Bock AS et al. (2017) The visual white matter: The application of diffusion MRI and fiber tractography to vision science. J Vis, 17(2):4

Rosa MGP, Palmer SM, Gamberini M, et al. (2009) Connections of the dorsomedial visual area: pathways for early integration of dorsal and ventral streams in extrastriate cortex. J Neurosci 29:4548–4563 [PubMed: 19357280]

Rosa MGP, Tweedale R (2005) Brain maps, great and small: lessons from comparative studies of primate visual cortical organization. Philos Trans R Soc Lond B Biol Sci 360:665–691 [PubMed: 15937007]

Sani I, McPherson BC, Stemmann H, et al. (2019) Functionally defined white matter of the macaque monkey brain reveals a dorso-ventral attention network. Elife 8: e40520 [PubMed: 30601116]

Schaeffer DJ, Adam R, Gilbert KM, et al. (2017) Diffusion-weighted tractography in the common marmoset monkey at 9.4T. J Neurophysiol 118:1344–1354 [PubMed: 28615334]

Schmahmann JD, Pandya D (2006) Fiber pathways of the brain. Oxford Univ Press, New York

Schmahmann JD, Pandya DN, Wang R, et al. (2007) Association fibre pathways of the brain: parallel observations from diffusion spectrum imaging and autoradiography. Brain 130:630–653 [PubMed: 17293361]

Schurr R, Filo S, Mezer AA (2019) Tractography delineation of the vertical occipital fasciculus using quantitative T1 mapping. NeuroImage 202:116121 [PubMed: 31472252]

Seltzer B, Pandya DN (1984) Further observations on parieto-temporal connections in the rhesus monkey. Exp Brain Res 55:301–312 [PubMed: 6745368]

Smith AT, Greenlee MW, Singh KD, et al. (1998) The processing of first- and second-order motion in human visual cortex assessed by functional magnetic resonance imaging (fMRI). J Neurosci 18:3816–3830 [PubMed: 9570811]

Solomon SG, Rosa MGP (2014) A simpler primate brain: the visual system of the marmoset monkey. Front Neural Circuits 8.: doi: 10.3389/fncir.2014.00096

Sotiropoulos SN, Jbabdi S, Xu J, et al. (2013) Advances in diffusion MRI acquisition and processing in the Human Connectome Project. Neuroimage 80:125–143 [PubMed: 23702418]

Sun SW, Neil JJ, Song SK (2003) Relative indices of water diffusion anisotropy are equivalent in live and formalin-fixed mouse brains. Magn Reson Med 50:743–748 [PubMed: 14523960]

Takemura H, Caiafa CF, Wandell BA, Pestilli F (2016a) Ensemble tractography. PLoS Comput Biol 12:e1004692 [PubMed: 26845558]

Takemura H, Pestilli F, Weiner KS, et al. (2017) Occipital white matter tracts in human and macaque. Cereb Cortex 27:3346–3359 [PubMed: 28369290]

Takemura H, Pestilli F, Weiner KS (2019) Comparative neuroanatomy: integrating classic and modern methods to understand association fibers connecting dorsal and ventral visual cortex. Neurosci Res 146:1–12 [PubMed: 30389574]

Takemura H, Rokem A, Winawer J, et al. (2016b) A major human white-matter pathway between dorsal and ventral visual cortex. Cereb Cortex 26:2205–2214 [PubMed: 25828567]

Tax CMW, Dela Haije T, Fuster A, et al. (2016) Sheet Probability Index (SPI): Characterizing the geometrical organization of the white matter with diffusion MRI. Neuroimage 142:260–279 [PubMed: 27456538]

Thiebaut de Schotten M, Dell'Acqua F, Forkel SJ, et al. (2011) A lateralized brain network for visuospatial attention. Nat Neurosci 14:1245–1246 [PubMed: 21926985]

Thiebaut de Schotten M, Dell'Acqua F, Valabregue R, Catani M (2012) Monkey to human comparative anatomy of the frontal lobe association tracts. Cortex, 48:82–96 [PubMed: 22088488]

Thiebaut de Schotten M, Cohen L, Amemiya E, et al. (2014) Learning to read improves the structure of the arcuate fasciculus. Cereb Cortex 24:989–995 [PubMed: 23236205]

Thiebaut de Schotten M, Croxson PL, Mars RB (2019) Large-scale comparative neuroimaging: Where are we and what do we need? Cortex 118:188–202 [PubMed: 30661736]

Thomas C, Ye FQ, Irfanoglu MO, et al. (2014) Anatomical accuracy of brain connections derived from diffusion MRI tractography is inherently limited. Proc Natl Acad Sci U S A 111:46

Tootell RB, Tsao D, Vanduffel W (2003) Neuroimaging weighs in: humans meet macaques in "primate" visual cortex. J Neurosci 23:3981–3989 [PubMed: 12764082]

Tournier JD, Calamante F, Connelly A (2012) MRtrix: Diffusion tractography in crossing fiber regions. Int J Imaging Syst Technol 22:53–66

Ungerleider LG, Galkin TW, Desimone R, Gattass R (2008) Cortical connections of area V4 in the macaque. Cereb Cortex 18:477–499 [PubMed: 17548798]

Ungerleider LG, Mishkin M (1982) Two cortical visual systems In: Ingle DJ, Goodale MA, Mansfield RJW (eds) The analysis of visual behavior. MIT Press, Cambridge, MA, pp 549–586

Van Essen DC, Glasser MF (2018) Parcellating cerebral cortex: how invasive animal studies inform noninvasive mapmaking in humans. Neuron 99:640–663 [PubMed: 30138588]

Van Essen DC, Smith SM, Barch DM, et al. (2013) The WU-Minn Human Connectome Project: an overview. Neuroimage 80:62–79 [PubMed: 23684880]

Vogt O (1904) Neurobiologische Arbeiten. Fischer

Wade AR, Brewer AA, Rieger JW, Wandell BA (2002) Functional measurements of human ventral occipital cortex: retinotopy and colour. Philos Trans R Soc Lond B Biol Sci 357:963–973 [PubMed: 12217168]

Wakana S, Jiang H, Nagae-Poetscher LM, et al. (2004) Fiber tract-based atlas of human white matter anatomy. Radiology 230:77–87 [PubMed: 14645885]

Wallisch P, Movshon JA (2008) Structure and function come unglued in the visual cortex. Neuron 60:195–197. [PubMed: 18957212]

Wandell BA, Winawer J (2011) Imaging retinotopic maps in the human brain. Vision Res 51:718–737 [PubMed: 20692278]

Wang Y, Fernández-Miranda JC, Verstynen T, et al. (2013) Rethinking the role of the middle longitudinal fascicle in language and auditory pathways. Cereb Cortex 23:2347–2356 [PubMed: 22875865]

Wedeen VJ, Rosene DL, Wang R, et al. (2012) The geometric structure of the brain fiber pathways. Science 335:1628–1634 [PubMed: 22461612]

Weiner KS, Yeatman JD, Wandell BA (2017) The posterior arcuate fasciculus and the vertical occipital fasciculus. Cortex 97:274–276 [PubMed: 27132243]

Winawer J, Horiguchi H, Sayres RA, et al. (2010) Mapping hV4 and ventral occipital cortex: the venous eclipse. J Vis 10:1

Woodward A, Hashikawa T, Maeda M, et al. (2018) The Brain/MINDS 3D digital marmoset brain atlas. Sci Data 5:180009 [PubMed: 29437168]

Wu Y, Sun D, Wang Y, et al. (2016) Tracing short connections of the temporo-parieto-occipital region in the human brain using diffusion spectrum imaging and fiber dissection. Brain Res 1646:152–159 [PubMed: 27235864]

Yeatman JD, Dougherty RF, Myall NJ et al. (2012) Tract profiles of white matter properties: automating fiber-tract quantification. PLoS ONE 7:e49790 [PubMed: 23166771]

Yeatman JD, Rauschecker AM, Wandell BA (2013) Anatomy of the visual word form area: adjacent cortical circuits and long-range white matter connections. Brain Lang 125:146–155 [PubMed: 22632810]

Yeatman JD, Weiner KS, Pestilli F, et al. (2014) The vertical occipital fasciculus: a century of controversy resolved by in vivo measurements. Proc Natl Acad Sci U S A 111:E5214–23 [PubMed: 25404310]

Yoshimine S, Ogawa S, Horiguchi H, et al. (2018) Age-related macular degeneration affects the optic radiation white matter projecting to locations of retinal damage. Brain Struct Funct 223:3889–3900 [PubMed: 29951918]

Zhu Q, Vanduffel W (2019) Submillimeter fMRI reveals a layout of dorsal visual cortex in macaques, remarkably similar to New World monkeys. Proc Natl Acad Sci U S A 116:2306–2311 [PubMed: 30674668]

Zilles K, Armstrong E, Moser KH, Schleicher A, Stephan H (1989) Gyrification in the cerebral cortex of primates. Brain Behav Evol. 34:143–150 [PubMed: 2512000]

Zilles K, Palomero-Gallagher N, Amunts K (2013) Development of cortical folding during evolution and ontogeny. Trends Neurosci. 36:275–284 [PubMed: 23415112]

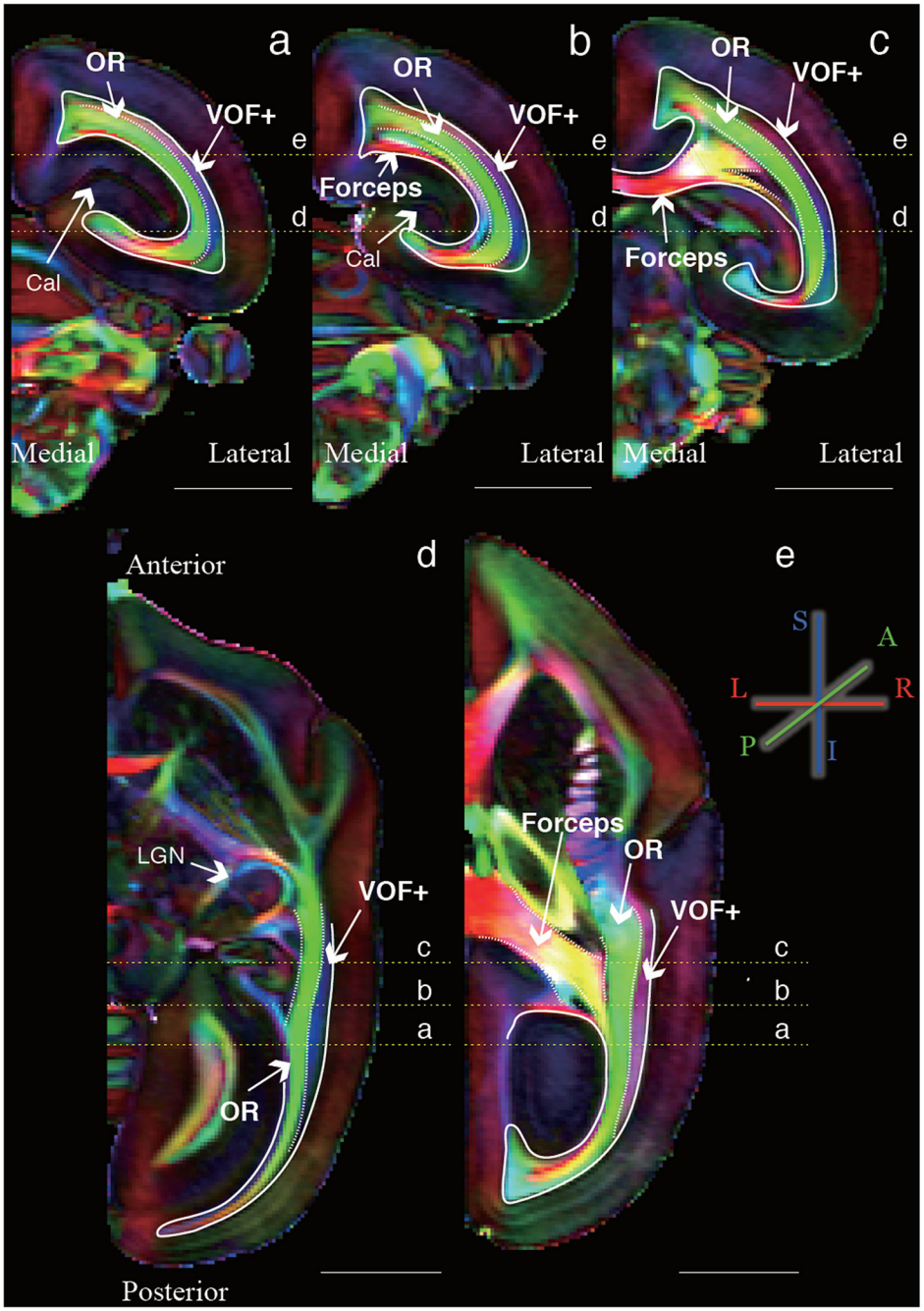

Figure 1. Major occipital white matter tracts in marmoset are visible in DEC maps from diffusion MRI data.

The color schema represents the principal diffusion direction in each voxel (red, left-right; green, anterior-posterior; blue, superior-inferior) in representative coronal (a-c; posterior to anterior) or axial slices (d-e; inferior to superior) of a marmoset brain (marmoset1). Scale bars in each panel indicate 5 mm. Yellow lines show the slice position presented in the other orthogonal slices. OR: optic radiation, Forceps: forceps major, VOF+: Vertical occipital fasciculus complex, Cal: Calcarine sulcus, LGN: Lateral geniculate nucleus.

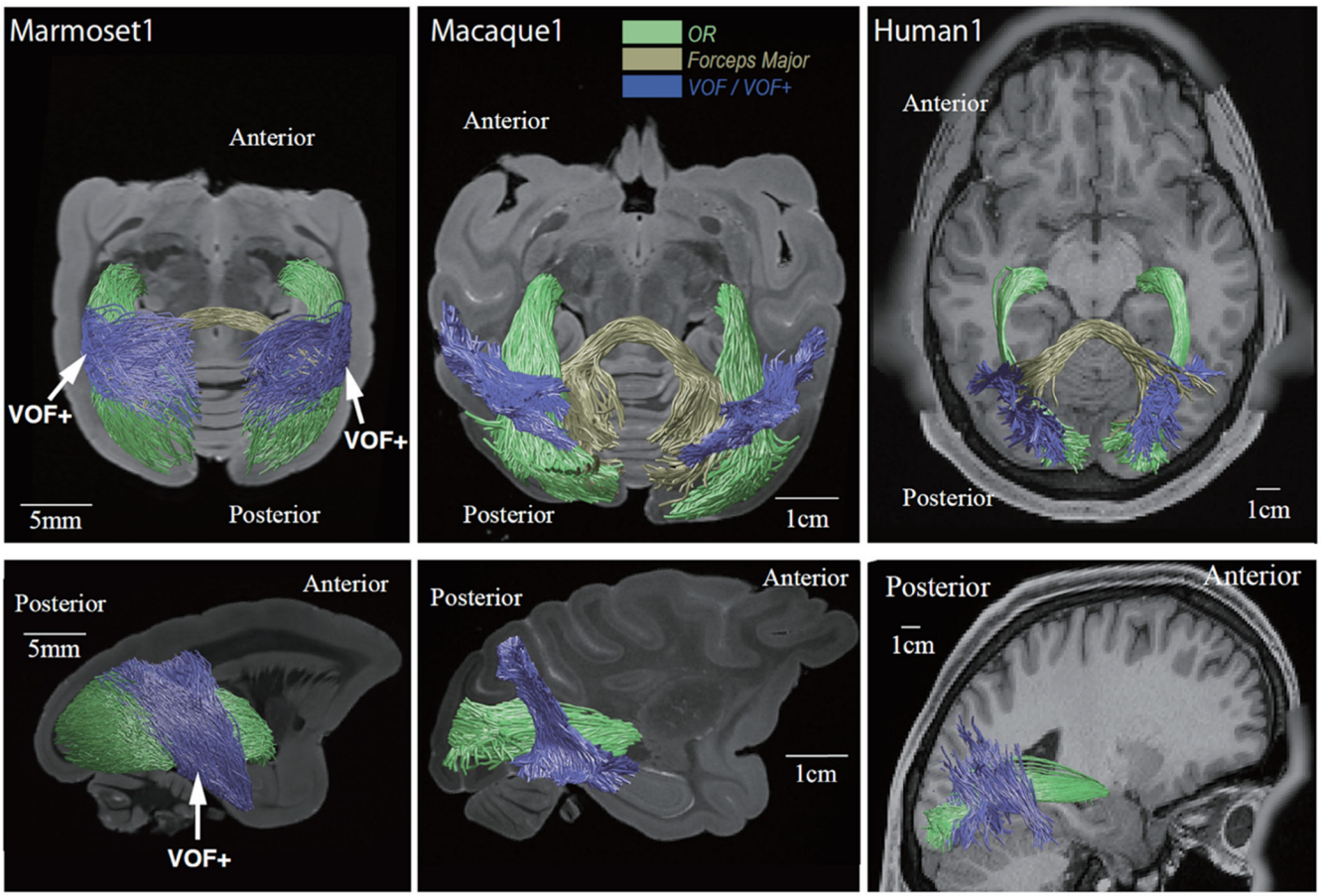

Figure 2. Tractography of three major occipital white matter tracts in marmoset, macaque and humans.

Axial (top panels) and sagittal view (bottom panels) of tractography overlaid on anatomical images in representative subjects for each of species. In all species, we identified the optic radiation (green), forceps major (dark yellow), and VOF/VOF+ (blue). Spatial scales differ across species and are indicated by the white bar in each panel.

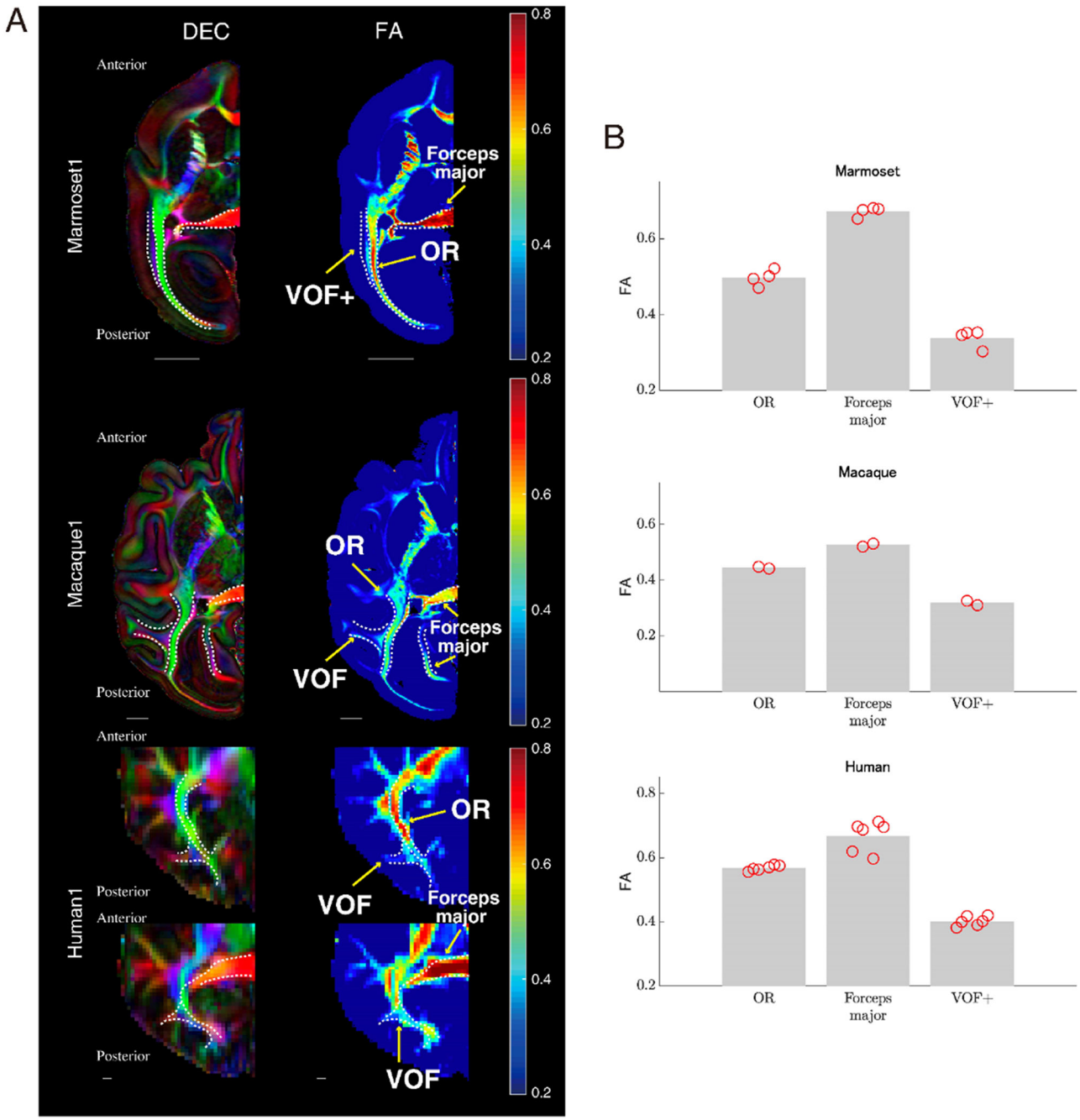

Figure 3. FA comparison across species along major occipital white matter tracts.

A. *Left panel*: Tract positions were (white dotted line) overlaid on axial slices of DEC maps of marmoset (top panel, marmoset1), macaque (middle panel) and human data (bottom panel, human1). *Right panel*: FA maps of the same axial slices as the left column. Color coding of FA maps is depicted in color bars on the right. The scale bar in each plot indicates 5 mm. **B.** Mean of FA value along each tract in marmoset (top panel), macaque (middle panel) and human data (bottom panel; see Methods section for the detail). Bars represent

averaged FA across hemispheres, while red circles depict FA of tracts in individual hemispheres.

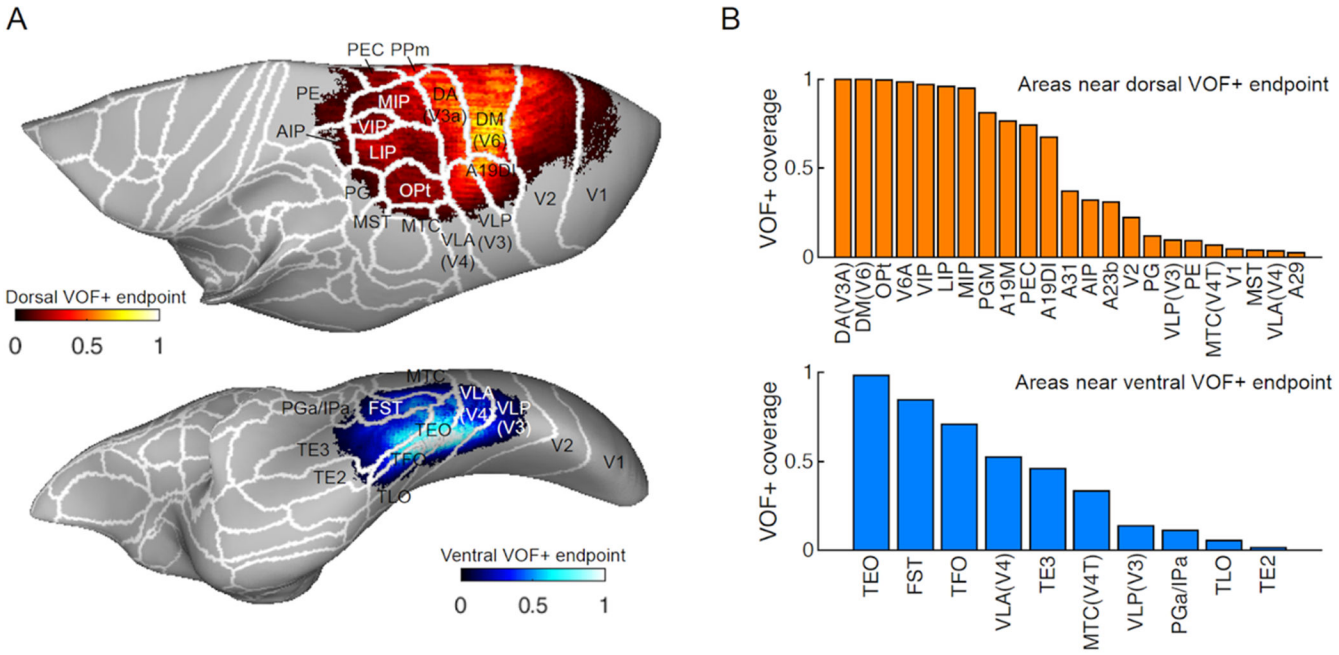

Figure 4. Putative cortical endpoints of marmoset VOF+ streamlines.

A. Normalized VOF+ streamline endpoint density (averaged across 4 hemispheres) represented over the cortical surface model of the marmoset brain atlas with cortical parcellations defined by comparisons between MRI and histology data (Hashikawa et al., 2015; Woodward et al., 2018). *Top panel*: Dorsal endpoint of marmoset VOF+. *Bottom panel*: Ventral endpoint of marmoset VOF+. The intensity of colors indicates normalized VOF+ streamline endpoint counts in each vertex (red, top panel; blue, bottom panel). **B.** VOF+ endpoints coverage of each cortical area for dorsal (top panel) and ventral endpoint (bottom panel), respectively. The vertical axis indicates proportions of voxels in each area which have normalized VOF+ streamline endpoint counts larger than 0.5. See Methods for further details in this analysis.

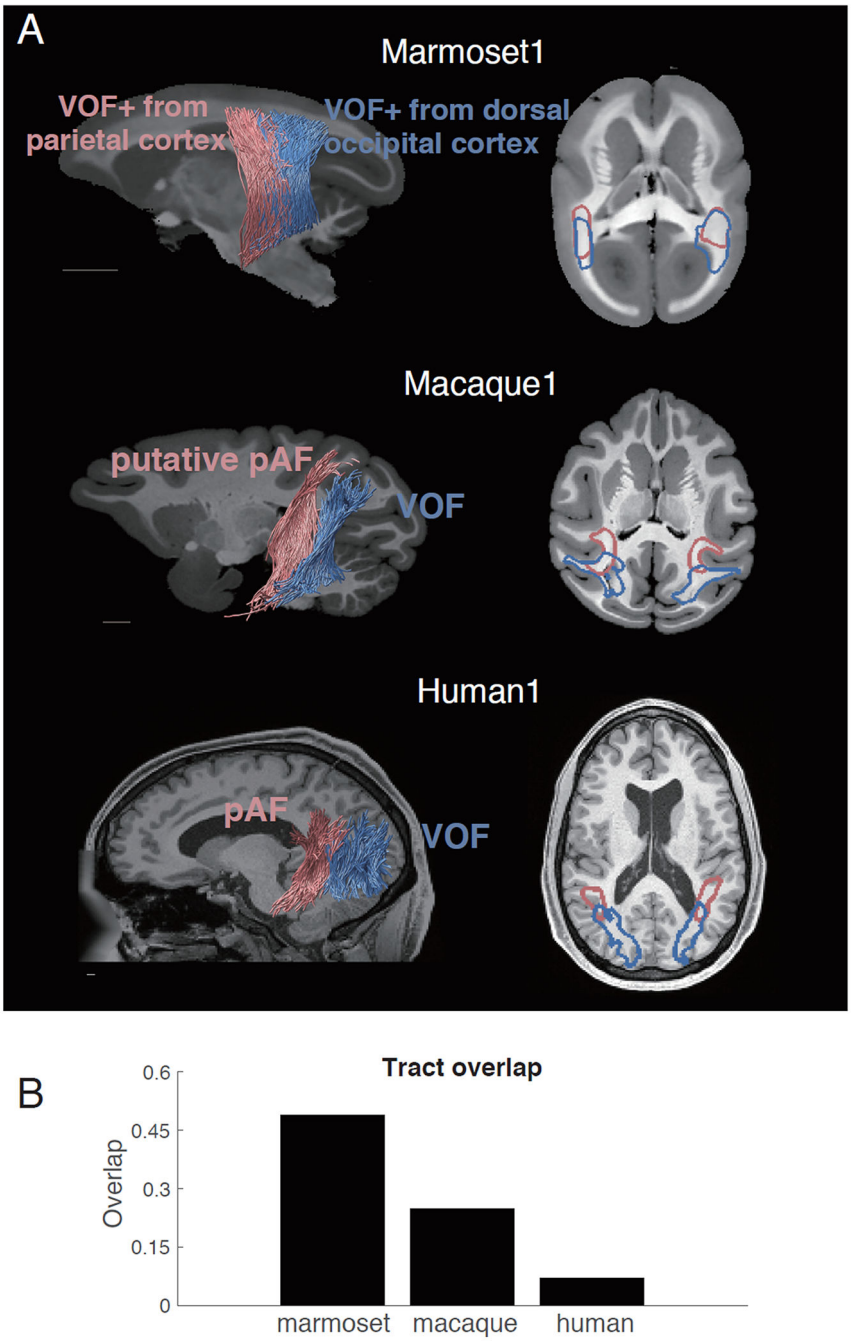

Figure 5. Comparison between marmoset VOF+ with pAF and VOF of macaque and human.

A. *Top left panel*: Marmoset VOF+ subdivided into anterior and posterior subcomponents. Red streamlines are VOF+ subcomponent with dorsal endpoints near posterior parietal cortex. Blue streamlines are the other VOF+ subcomponent with dorsal endpoints near dorsal occipital cortex. *Middle and bottom left panels*: Macaque (middle) and human (bottom) pAF and VOF. Red streamlines are pAF and blue streamlines are VOF. *Right panels*: The positions of each fasciculus or subcomponent were shown as red or blue contours and are overlaid on an axial slice of the structural image. Unlike those in macaque

and human, two VOF+ subcomponents in marmoset (top right panel) did not exhibit a clear separation. The scale bars indicate 5 mm. **B.** The proportion of voxels in which two fasciculi overlap in marmoset, macaque and human. While this plot is based on single subject for each species, we note that results are highly consistent in another marmoset brain and other human datasets.